

Recent Advances in Sawtooth Control

J. P. Graves^{1*}, I. T. Chapman², S. Coda¹, T. Johnson³, M. Lennholm⁴, J. I. Paley¹, O. Sauter¹ and JET-EFDA Contributors[†]

JET-EFDA, Culham Science Centre, OX14 3DB, Abingdon, UK.

¹ *École Polytechnique Fédérale de Lausanne (EPFL), Centre de Recherches en Physique des Plasmas, Association EURATOM-Confédération Suisse, 1015 Lausanne, Switzerland*

² *Euratom/CCFE Fusion Association, Culham Science Centre, Abingdon, UK*

³ *Euratom-VR Association, EES, KTH, Stockholm, Sweden*

⁴ *EFDA-JET CSU, Culham Science Centre, Abingdon, OX14 3DB, UK*

Abstract

Important advances have been made recently in the invention and application of experimental methods to control the sawtooth instability in tokamak plasmas. The primary means of control involves the application of either ion cyclotron resonance heating, or electron cyclotron heating, with resonance very close to the $q = 1$ radius in the plasma core. Reported here are experiments which have successfully applied these methods in order to either shorten or lengthen the sawteeth deliberately, in a variety of plasma conditions, in three tokamaks: JET, TCV and TORE-SUPRA. It is shown that despite the sensitivity of the sawtooth period to the resonance position, sawteeth can be controlled using either real-time control of the electron cyclotron

*jonathan.graves@epfl.ch

[†]See the Appendix of F. Romanelli et al., Fusion Energy Conference 2008 (Proc. 22nd Int. FEC Geneva, 2008) IAEA, (2008)

deposition, or in the case of ion cyclotron heating, very careful adjustment of the magnetic field strength and minority ion concentration. The latter technique has been guided by theoretical advances which have enabled the control of sawteeth in JET with ITER relevant ICRH scenarios.

Keywords: sawtooth control; electron cyclotron current drive; toroidally asymmetric fast ion distributions

I. INTRODUCTION

The need for effective control of sawteeth has been well documented over the last few years. Due to the stabilising role of trapped alpha particles, sawteeth are expected to be strongly stabilised in ITER [1] leading to long cyclic intercrash times (sawtooth period). Of particular concern is that interaction between large sawteeth and neoclassical tearing modes (NTM's) has been observed [2–4] in the Joint European Torus (JET) [5], while discharges with smaller regular sawteeth are typically found to have increased core confinement, and are less likely to be coupled to confinement degrading NTM's. Hence greater understanding and eventual control over the mechanisms that determine sawtooth stability is required.

This contribution aims to review the primary recent advances in the application of sawtooth control methods in tokamaks. Over recent years there has been renewed interest in the theoretical understanding of sawteeth, and the experimental implementation of control techniques. In these studies, control refers to the objective of deliberately manipulating the period of sawteeth, and usually the objective is to shorten it. An important advance has been to show that energetic ions have a significant, and moreover, a controllable effect on the stability of the internal kink mode, thought to underlie the sawtooth phenomenon. **It has long been known that, for example, ICRH can be employed to modify sawteeth, including deliberate shortening of them [6–8]. Previously, it was thought that the the sawteeth were modified due to the change in the local magnetic**

shear arising from the local heating and phasing of the antenna. While magnetic shear can play a role in many scenarios, as developed in some detail in Ref. [9], it has recently been shown [10,11] that passing fast ions with a large orbit widths also strongly influence sawtooth stability, due to the radial drift excursion of the energetic ions which are distributed asymmetrically in the velocity parallel to the magnetic field. These effects from fast ions should not be confused with the established stabilising effect of trapped fast particles (e.g. [2,12,13]), whose effects also play an important role in determining stability. The asymmetric distributions that lead to the passing ion effects described in Refs. [10,11] occur naturally when unbalanced neutral beams are applied [14], or ICRH is employed with asymmetric antenna phasing [15,16]. Analytical techniques [10,11] and numerical modelling [11,17] have enabled not simply interpretation of observations, but the prescription of conditions required for the desired sawtooth period.

There have been notable advances in sophisticated experimental control techniques. Recent results exhibiting control of sawteeth by steerable electron cyclotron resonance heating (ECRH) in TCV [18] and TORE-SUPRA [19] have included real-time feedback schemes and robust control of the magnetic shear via electron cyclotron current drive (ECCD) and localised heating. Moreover, dramatic changes in sawtooth stability have also been achieved in JET [20] by the application of off-axis ICRH with toroidally asymmetric antenna phasing. Consistent with theory [11], ICRH has been shown to control sawteeth due to kinetic effects even under conditions where the modification to the magnetic shear is minimised [20]. It is concluded that various robust control schemes have been established, and ever more sophisticated analytic and numerical modelling are helping define the requirements of sawtooth control actuators in ITER. Other notable advances not discussed in this paper include sawtooth control using lower hybrid [21] and mode conversion techniques [22]. A summary of these contributions and some of those discussed in this document will be reviewed in due course [23].

This paper starts in section II with a brief overview of the stability criteria of the internal kink which is widely used to interpret and design experiments. In section III we report real-time techniques in TCV which aimed to manipulate the sawtooth period via ECCD. In section IV similar techniques employed in TORE-SUPRA are shown, but with the primary difference being that the control techniques functioned despite a fast ion population in the core which originally lengthened the period. In section V, simulations are shown predicting the contribution of driven current from the planned upper EC launcher of ITER on the q profile and shear. In section VI we report experiments in JET which have exploited neutral beam ion (NBI) deposition in order to control sawteeth in JET, while section VII reports recent experiments employing ICRH with ITER-relevant minority ^3He in order to control sawteeth. Summarising remarks are to be found in section VIII.

II. THE THEORY OF THE SAWTOOTH TRIGGER

The sawtooth trigger problem is addressed by seeking to correlate equilibrium properties at the onset of the $m = n = 1$ instability with the crossing of a theoretical stability boundary for the internal kink mode. The theoretical boundary differs as additional physical effects are added into the linearised ‘MHD’ equations. It is generally found that the sawtooth period further increases with increasing heating power. Such a dependence on heating is consistent with the sawtooth trigger being described by resistive MHD with two fluid effects [24]. Although the $m = n = 1$ instability is always unstable in one-fluid resistive MHD, accounting for two fluid effects in the singular layer around $q = 1$ reveals stable regions of parameter space which might account for quiescence during sawteeth [25]. The instability criteria can be written in the form $s_1 > s_c(\beta)$. In Ref. [26] argued that the effects in the layer, which are described by the latter critical shear criterion, are only important when the macroscopic drive $\delta\hat{W}$ of the internal kink mode is not strongly stabilising, i.e. there is not a very large energy sink. Basing the stability criteria on a combination of these ideas one obtains the following condition for instability [26]:

$$\pi \frac{\delta \hat{W}}{s_1} < c \hat{\rho} \quad (1)$$

and

$$s_1 > s_c(\beta), \quad (2)$$

where $\hat{\rho}$ is the ion Larmor radius normalised to the $q = 1$ radius, c a numerical constant of order unity, and s_c is a critical shear governed essentially by the pressure profile [26,25,27]. The ideal growth rate $\gamma\tau_A = -\epsilon_1^2 \pi \delta \hat{W} / s_1$, so that $\delta \hat{W} = \delta W / (2\pi^2 \xi_0^2 \epsilon_1^2 R_0 B_0^2 / \mu_0)$. The definition of s_c depends on the regime of interest [28]. In large tokamaks with significant heating, s_c is governed by instability in the ion kinetic regime, while in smaller machines it is governed by resistive instability. Nevertheless, s_c increases monotonically with plasma beta, and it is typically found [28] that $s_c \approx 0.2$ close to the sawtooth crash threshold. In section III and IV the sawtooth trigger condition will be understood in terms of the impact of a manipulation in the shear, via electron cyclotron current drive, on the thresholds of Eqs. (1) and (2). Furthermore, in the TORE-SUPRA pulse described section IV, ICRH ions initially stabilise the sawteeth via the stabilising trapped ICRH ion contribution to $\delta \hat{W}$ in Eq. (1), but as shown in Ref. [19], ECCD can nevertheless sufficiently modify the shear in order to trigger sawteeth. For the simulations of the expected current drive in ITER, illustrated in section V, it is found that ECCD should be capable of enhancing the magnetic shear at $q = 1$ to around 0.4. It is anticipated that this enhancement in the shear is sufficient to trigger sawteeth in the presence of a large alpha particle population, which is expected to create a very large stabilising $\delta \hat{W}$ in e.g. Eq. (1).

To leading order in accuracy, kinetic contributions to $\delta \hat{W}$ contribute to stability in an additive fashion, and thus do not affect the essential form of the MHD contribution to stability δW_{MHD} nor the overall structure of the stability criterion of Eq. (1). Important kinetic effects arise from asymmetrically distributed passing particles with finite orbit widths. Both unbalanced NBI [10,17] and toroidally propagating ICRH [11,20] yield such populations, and their distributions can be manipulated in such a way so as to deliberately affect stability. In

ITER, $\delta\hat{W}$ is expected to be very large and positive due to the stabilising effect of trapped fusion alpha particles, whilst $\hat{\rho}$ will be much smaller than in most present day experiments. Consequently, in ITER, an actuator will have to generate a large change in s_1 in order to satisfy Eq. (1). By contrast, the fast ion mechanism proposed in Refs [10,11] generates a decrease in the macroscopic energy of the internal kink mode due to either ‘NBI’ or ‘RF’ ions, and as a result, it is envisaged that the criterion for instability (e.g. (1)) can be met even when there is a significant stabilising trapped ion population in the core, and especially in conjunction with enhanced s_1 , via e.g. an additional ECCD actuator. JET evidence of direct control of sawteeth with fast ion kinetic effects is shown in section VI and VII. In section VI the control is via neutral beam injection, while in VII the control is via ICRH. The mechanism can be understood with the aid of Fig. 1, which is reproduced from Ref. [29]. Passing ion orbits with wide orbit widths are illustrated. Due to the top-hat structure of the internal kink mode, particles only contribute to mode stability when their orbits are within the $q = 1$ radius. Consequently, for particles that happen to intersect $q = 1$, only the portion of the orbit that is inside $q = 1$ will contribute to stability. Whether such a particle is stabilising depends on whether such a particle is inside $q = 1$ on the region of good curvature or poor curvature. It turns out that this depends on the sign of the parallel velocity of the single passing particle. A net effect requires an asymmetry in the parallel velocity of the distribution function F . Moreover, stability also depends on the radial gradient of the distribution function. In general, destabilisation occurs when $\partial F(v_{\parallel} > 0)/\partial r > \partial F(v_{\parallel} < 0)/\partial r$. Destabilisation will therefore occur for off-axis NBI ($\partial F/\partial r > 0$) with injection orientated along the plasma current ($F(v_{\parallel} > 0) > F(v_{\parallel} < 0)$), or with on-axis beams ($\partial F/\partial r < 0$) with injection orientated counter to the plasma current ($F(v_{\parallel} > 0) < F(v_{\parallel} < 0)$). Both of these combinations of unbalanced NBI are demonstrated to destabilise sawteeth in section VI. This mechanism also explains the control of sawteeth using toroidally propagating ICRH, with resonance close to the $q = 1$ radius. Nevertheless, for a given antenna phasing, the ratio of the number of co and counter passing ions depends sensitively on radial position

relative to the resonance radius. Thus a given antenna phasing can be stabilising or destabilising to sawteeth, depending sensitively on the resonance position relative to the $q = 1$ surface. In section VII recent JET experiments are described briefly which aim to verify the control mechanism, and minimise the effect of ICRH on the current profile. Without such experiments, it could be argued that sawtooth control occurred because of a magnetic shear change, as in ECCD experiments of TCV [30,18] and TORE-SUPRA [31,19]. **Finally, it should be pointed out that despite the apparent applicability of asymmetric NBI and RF distributions to control sawteeth in ITER, there is a downside. The ratio of finite orbit width to minor radius, for a given representative single particle energy, is lower in ITER than it is in JET. As a result, the ability of the asymmetric passing ion population to compete with the stabilising effect of trapped fast ions is reduced. The ratio of these contributions to δW is proportional to ratio of finite orbit width to minor radius (see e.g. Eq. (9) of Ref. [10]), which is reduced by about a factor of one quarter in ITER compared to JET.**

FIGURES

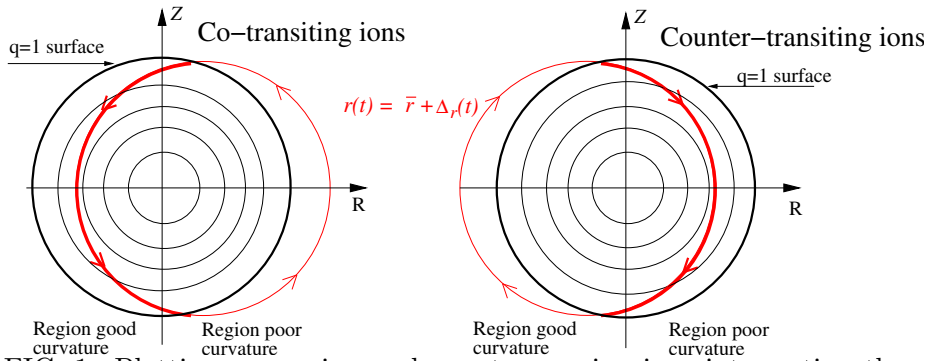


FIG. 1. Plotting co-passing and counter passing ions intersecting the $q = 1$ surface. Figure reproduced from [J. P. Graves, *et al* Phys. Plasmas **17**, 056118 (2010), Copyright 2010 Euratom].

III. REAL-TIME CONTROL OF SAWTEETH USING ELECTRON CYCLOTRON CURRENT DRIVE IN TCV

The 2nd harmonic X-mode (82.7 GHz-X2) EC heating system at TCV (major radius 0.88 m, max toroidal field = 1.5 T, max current = 1 MA) consists of 6×0.5 MW gyrotrons with individual launchers. Each launcher is rotated about its longitudinal axis (inter-shot) to change the parallel wave number (i.e. changing between ECRH and ECCD). The final launcher mirror rotates to control the location of the poloidal deposition; however, in general this motion also affects the current drive. It is the poloidal angle of this final mirror that is controllable in real-time.

In order to build a real-time control system, it is desirable to have a model of the sawtooth response to movements in the EC launcher injection angle which can be used to develop and test the control algorithm. Figure 2 shows a plot of the sawtooth period in response to feedforward sweeps of EC deposition across the $q = 1$ surface [18]. One EC beam was used to modify the shear. As well as modifying the local current profile, movement of the EC beam causes a redistribution of the global plasma current on a slower timescale, which manifests itself as hysteresis in the peak of the sawtooth period when the EC beam is swept across the $q = 1$ surface in the subsequent reverse direction. Off-axis deposition broadens the global current profile, shrinking the $q = 1$ surface, whereas core deposition peaks the

current profile, moving the $q = 1$ surface to a larger radius. The result of the feedforward sweep was used to generate a lookup table of the launcher angle versus sawtooth period. In Fig. 2 is shown the sawtooth period as a function of varying launcher angle, using co-current ECCD/ECRH.

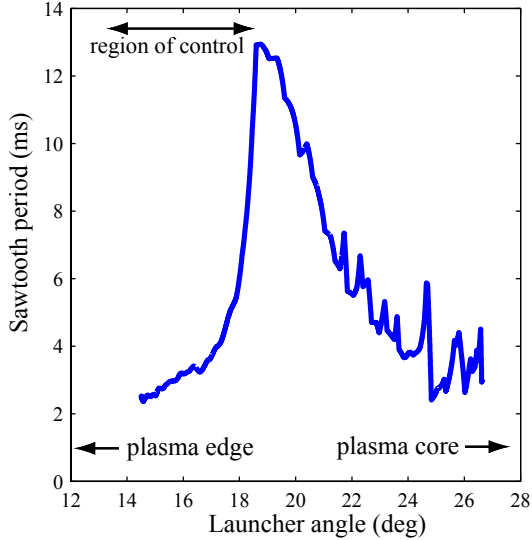


FIG. 2. Showing the variation of the sawtooth period in TCV pulse 35807 as the poloidal angle of the EC launcher moves the resonance position.

The algorithms developed in Ref. [18] rely exclusively upon the detected response of the sawtooth period to movements of the launcher and required the deposition to be targeted off-axis, outside the $q = 1$ surface (or more accurately outside the peak in the sawtooth period). In this case the controller moves the launcher to a larger angle in order to increase the sawtooth period and to a smaller angle for a shorter period, although alternatively, the deposition could be targeted for the plasma core, in which case the controller gains would be reversed. The central philosophy is to generate sawteeth of a pre-determined period, with the target reference period typically varying in time.

An example [18] of the closed loop real-time control of sawteeth in TCV is shown in Fig. 3. The initial target sawtooth period of 3ms is obtained within 0.15ms of the activation of the controller. Next, a step change in the target is demanded, and it is seen that the new reference of 8.5ms is obtained within around 0.4s, and the target is maintained for the

duration of the activation phase of the pulse. Similar real-time control techniques to those shown here in TCV have been implemented recently in JET, using ICRH frequency control to move the resonance position [32].

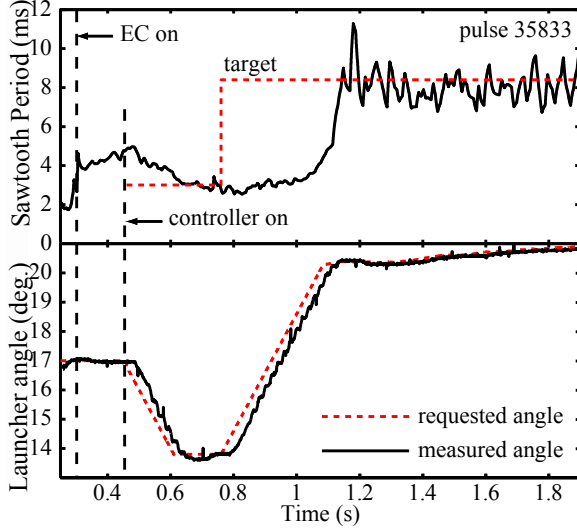


FIG. 3. The real-time control of the launcher angle is activated at $t=0.45$ s in TCV pulse 35833.

A target period of 3ms is obtained within 400ms of the controller being activated. The target period of 8.5ms is later achieved and tracked. Figure reproduced from Ref. [J. I. Paley , *et al*, Plasma Phys. Control. Fusion **51**, 124041 (2009), copyright 2009 IOP publishing].

IV. REAL-TIME CONTROL OF FAST ION LENGTHENED SAWTEETH USING ELECTRON CYCLOTRON CURRENT DRIVE IN TORE-SUPRA

The experiments reported in this section were carried out on the Tore Supra tokamak (major radius: 2.4 m, minor radius: 0.8 m) using a toroidal field of 3.8T, and a plasma current of 1 MA. Similarly to previous JET experiments of Refs. [33,34], central ICRH (57 MHz) was used to create a significant central pressure of fast ions with energies in the MeV range. The effect of O-mode ECH with co- and counter-ECCD on the sawtooth period has been explored in discharges where the Tore Supra ECCD system was capable of varying toroidal and poloidal injection angles over a wide range in order to sweep the ECCD deposition from outside the $q = 1$ surface, to inside, and towards the plasma center.

To explore the robustness of these results, the experiments reported in Ref. [19] were repeated at different values of ICRH power and plasma density. Sawtooth destabilization was achieved for the full range of available ICRH powers (0 to 4 MW) and over a wide range of densities. Despite the modest amount of ECCD power (300kW) a very strong and systematic effect on the sawtooth period was observed in all cases. When the ECCD power was deposited in a fairly narrow range around the $q = 1$ surface the sawtooth period abruptly switched from ICRH stabilised long sawteeth to short sawteeth with a period near the ohmic sawtooth period. When ECCD was deposited outside the destabilisation region the sawtooth period was virtually unaffected by the ECCD. Following the experiments in which the ECCD location was swept across the $q = 1$ surface, real-time sawtooth period control was implemented. Given the abrupt change between short and long sawteeth, the simple feedback controller which was implemented initially resulted, unsurprisingly, in an oscillatory behaviour, with the sawtooth period switching periodically between short and long sawteeth. As the aim of real-time sawtooth control is to maintain short sawteeth such an oscillatory behaviour is not acceptable. For this reason an alternative 'search and maintain' control algorithm was implemented. In this algorithm, not only the sawtooth period but also the sawtooth inversion radius was determined in real-time. When this algorithm became active the control proceeded in three stages as indicated by the three shaded regions of Fig. 4. Initially (during phase I of Fig. 4) the ECCD position was varied until the sawtooth period was shorter than a target value. During the second phase (phase II in Fig. 4), the mirror movement was halted and the sawtooth inversion radius and the ECCD location were recorded to determine the distance between inversion radius and ECCD location at which destabilisation is achieved. Since the distance found in this manner is only marginally inside the destabilising region, 2 cm was added to the reference distance in order to reliably maintain short sawteeth. In phase III of Fig. 4, a closed loop PI controller maintains the distance between the ECCD location and the inversion radius, and ensures that it is at the reference distance determined in phase two. In contrast to the algorithm used in TCV (section III), in the algorithm used here in TORE-SUPRA it is not necessary

to know the absolute position of ECCD as a function of mirror position, nor to pre-calculate a look-up table relating mirror angle and sawtooth period. The only information required in advance is the mirror rotation required to move the ECCD by a certain distance. A linear approximation, giving the number of cm the ECCD location moves when the mirror angle is moved by 1 degree is sufficient and this is easily determined a priori through ray-tracing calculations. Figure 4 shows that the position where short sawteeth are achieved is rapidly found, and subsequently these short sawteeth are maintained throughout the pulse despite the presence of fast ions in the core. Assuming that the abrupt transition observed in these experiments is typical for fast ion lengthened sawteeth as observed on Tore Supra and on JET, an advanced feedback controller along the lines of the Tore Supra controller will be required in ITER in order to maintain short sawteeth. In an ITER discharge, initiation of the controller would be required early in a pulse while the sawtooth period has not become too long. It is anticipated that this should allow short sawteeth to be maintained throughout the pulse by following the evolution of the $q = 1$ surface while heating and alpha power increases.

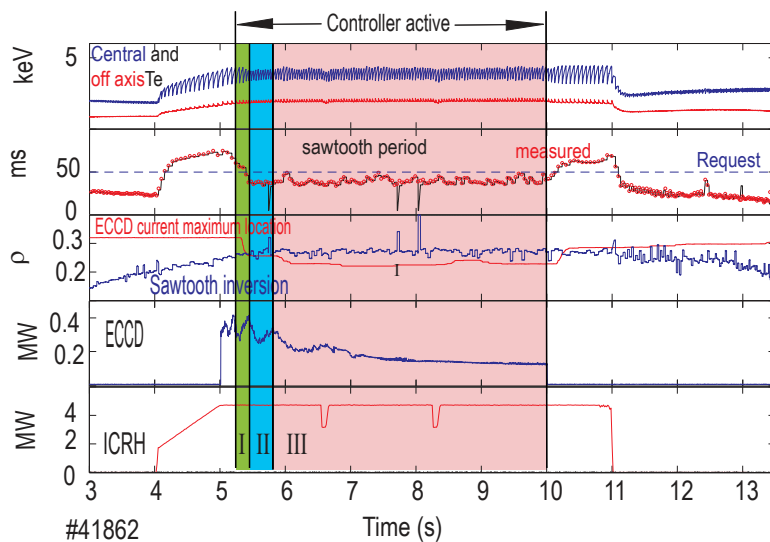


FIG. 4. Showing the successful implementation in TORE-SUPRA of active real-time feedback control on sawtooth period, via control of the EC launcher angle. Prior to the ECH phase the ICRH ions lengthen the sawtooth period.

V. CALCULATIONS OF MAGNETIC SHEAR CONTROL VIA THE ECH UPPER LAUNCHER IN ITER.

The original design of the ITER upper launcher [1] was intended uniquely for Neoclassical Tearing Mode (NTM) stabilization (and heating), by off-axis co-ECCD. As we have seen already, sawtooth period control can be achieved with the help of non-inductive current drive, via a change in the magnetic shear profile. Since the stabilizing effect of the fast particles scales inversely with the values of s_1 , it is hoped that a similar control can be obtained in ITER. Indeed, the TORE-SUPRA results [19] shown in section IV demonstrate that sawtooth control, via control of the magnetic shear, can be effective when fast particles initially stabilise the sawteeth. An optimized and enhanced upper launcher design [35] can drive co-ECCD at different radial locations inside the plasma and is therefore suitable for the purpose of sawtooth control. Thus, it is important for ITER to identify the effects of localized heating and current drive by EC waves on the total current density, and to infer an effect on the sawteeth.

Figure 5 (a) shows the total current density, including ECCD profiles corresponding to various ECH resonance locations [36]. **The ECH power is 6.6MW, which is one third of the total available power from the launcher, thus allowing additional heating of control elsewhere. Moreover, the driven current has had time to fully diffuse (i.e. reached steady state).** Figure 5 (b) and(c) also show the corresponding q and s profiles respectively. The original profile without ECCD is plotted in dashed-black and the circles indicate the position of the $q = 1$ surface. Without ECCD, the value of the magnetic shear at $q = 1$ is 0.15, which turns out to be a typical value expected at a sawtooth crash in present experiments in the absence of fast particle stabilisation. Gaussian profiles of co-ECCD driven by the revised upper launcher provided a total ECCD current of about 100-130kA. In Fig. 5(c) it is seen that by depositing co-ECCD inside or outside the $q = 1$ radius, the shear at $q = 1$ spans a rather large range, from 0 to 0.4. The increase in s_1 from the nominal value of 0.15 is about a factor of 2. It is envisaged that this modification

should allow stabilization of sawteeth with $0 < s_1 < 0.2$, or at least a significant increase of the period with consequent delay of the first sawtooth crash. In contrast, the increase in s_1 with the addition of co-ECCD inside the deposition radius should enable destabilisation of sawteeth. Note that if the deposition location is far outside the $q = 1$ surface, there is no significant effect on the shear at the $q = 1$ location, and the s_1 value stays approximately constant around 0.15 (red-blue-black lines from right in the shear plot). By moving the deposition inwards, the s_1 value drops rapidly to about 0 (yellow line in shear plot), and if the deposition is moved still further inward, the shear then rapidly starts increasing (cyan line in the shear plot) and finally stays constant at around 0.4 even if we keep on moving towards the magnetic axis (magenta-green-red-blue lines on the shear plot). This sensitive variation of the shear with resonance position is clearly similar to that observed in TCV [30] and TORE-SUPRA [19], and therefore it is hoped that real-time control of the ECH deposition in ITER to control the period will be equally successful.

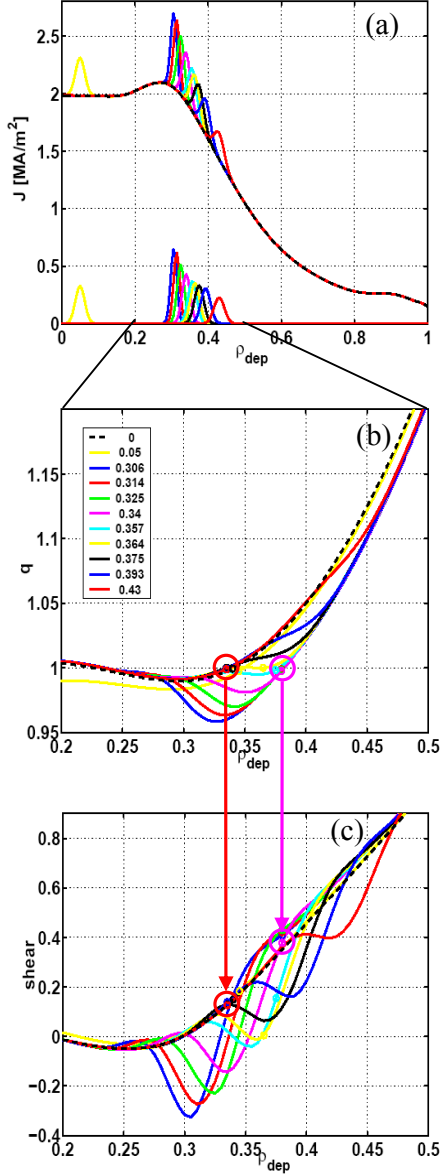


FIG. 5. Showing (a) the equilibrium current density profile for an ITER standard scenario, together with realistic current perturbations corresponding to various local depositions of the current drive from the enhanced electron cyclotron upper launcher design. Showing in (b) and (c) respectively, the change to the q -profile and the magnetic shear profiles corresponding to the current densities shown in (a). See Ref. [Zucca C 2009 PhD Thesis EPFL, no 4360 <http://library.epfl.ch/en/theses/?nr=4360>] for more detail.

VI. SAWTOOTH CONTROL WITH UNBALANCED NEUTRAL BEAM INJECTION

The possibility of using off-axis NBI as a sawtooth control actuator has been investigated experimentally and through stability analysis. The JET pulse 58855 reproduced in Fig. 6 from Ref. [37] shows that sawtooth oscillations are considerably more unstable when the plasma is heated with co-directed off-axis NBI than with on-axis NBI. Such a configuration corresponds to the conditions ($\partial F/\partial r > 0$) and $F(v_{\parallel} > 0) > F(v_{\parallel} < 0)$ as described in the introduction. Furthermore, the application of NBI heating deposited off-axis can destabilize sawteeth which had previously been strongly stabilized by **co-current** on-axis NBI heating. Clearly, this is explained qualitatively through the role of the passing ions in determining the stability of the $n/m = 1/1$ internal kink mode [10]. In JET the sawtooth behaviour is dominated by fast ion effects as the off-axis neutral beam current drive is weak and broadly deposited. In the experiments reported in [17], the total beam power is kept constant when the off-axis power is applied in order to keep the fast ion content the same, and to minimise the effect on the ideal mode stability. However, in order to demonstrate the suitability of off-axis co-NBI as a control tool, it is shown that ancillary application of off-axis beams is able to result in destabilization of otherwise strongly stabilized sawteeth. By applying on-axis NBI throughout the discharge in order to stabilize the sawteeth, the sawtooth behaviour under simultaneous application of off-axis NBI is an appropriate test of the use of off-axis beams as a sawtooth control mechanism [37]. The sawtooth period in Fig. 6 is substantially lengthened during the on-axis only phase (.315 ms) before decreasing to approximately the period of Ohmic sawteeth when the off-axis power is applied (.120 ms), but with the total applied power is held constant. This clear destabilization of the sawteeth when off-axis NBI is applied is also demonstrated in other JET discharges [17]. Furthermore, if the sawtooth behaviour is compared between 16s and 20s when there is constant on-axis power, then it is evident that the additional application of off-axis NBI can be used to destabilize long sawteeth. The sawtooth period decreases by a factor of 2 when the off-axis NBI is applied,

even though the total NBI power and fast ion pressure increases after 20s.

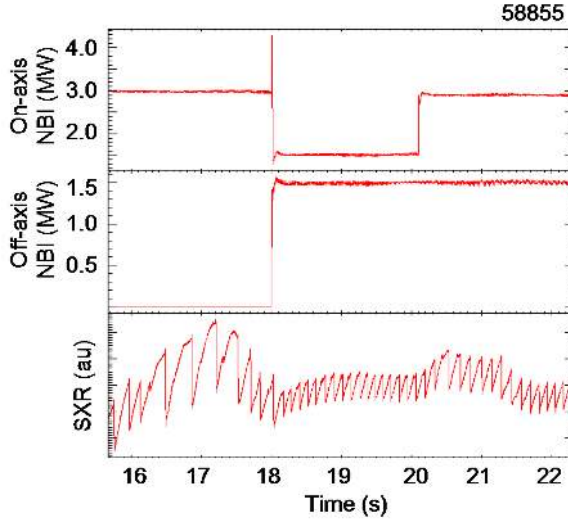


FIG. 6. The soft-x ray and NBI power for JET shot 58855. The sawtooth period is shorter when off-axis NBI is used in place of on-axis heating. Moreover, using off-axis heating can reduce the sawtooth period relative to a purely-on axis phase with smaller total auxiliary heating, and thus high hot ion (and plasma) beta. Figure reproduced from [I.T.Chapman *et al*, Nucl. Fusion 49 (2009) 035006, copyright 2009 EURATOM].

It is also possible to deliberately destabilise sawteeth with on-axis NBI, but with the orientation of the beams counter to the plasma current [38,39]. Such a configuration corresponds to the conditions $(\partial F/\partial r < 0)$ and $F(v_{\parallel} > 0) < Fv_{\parallel} < 0)$ as described in the introduction. In JET, these conditions were achieved during a reverse field campaign, where it was shown [38,39] that sawteeth could be destabilised, even relative to Ohmic sawteeth by the application of moderate power of the order of 4MW. The pulses shown in Fig. 7 summarise the variation of the sawtooth period with respect to the orientation and power of on-axis NBI in JET. Similar trends to that shown in Fig. 7 have been observed in MAST [40] and TEXTOR [41]. **In these JET pulses, it was necessary to have 7MW of ctr-NBI power in order to create sawteeth that were as long as those of Ohmic sawteeth.** But even 8MW of counter on-axis NBI yields sawteeth that are much shorter than sawteeth observed with 4MW of co on-axis NBI. It should be mentioned that there are

other effects that could play a role in the sawtooth period in addition to the finite orbit width effects discussed in the introduction. While it is argued that the current drive effects are probably negligible, the effect of plasma rotation on the kinetic response of trapped thermal and NBI ions could be important. Such effects have been derived and given due attention in various publications, e.g. [42,43,37], and indeed, such effects must be included [44] in order to explain the minimum of the sawtooth period in the counter-NBI regime observed in the JET experiments illustrated in Fig. 7 .

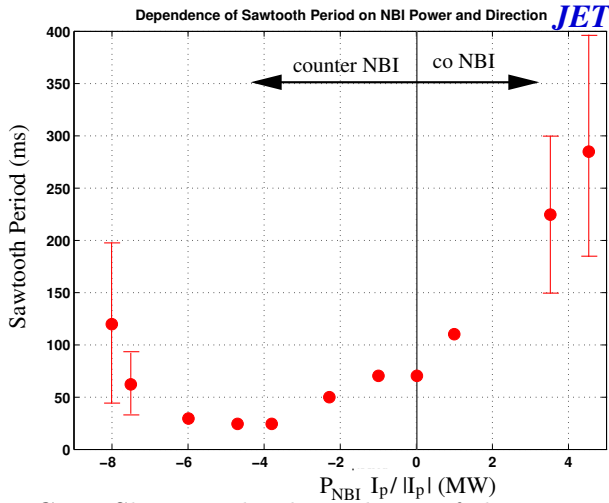


FIG. 7. Showing the dependence of the sawtooth period on NBI heating power and direction relative to the plasma current in a series of dedicated JET discharges. Error bars indicate variation of sawtooth period over the measured two second interval during which measurements were taken. Figure reproduced from [J.P.Graves *et al*, Plasma Phys. Control. Fusion 47 (2005) B121, copyright 2005 IOP publishing].

VII. ICRH EXPERIMENTS IN JET USING MINORITY ^3He

In this section it is shown that it is possible to control sawteeth with localised ICRH. In order to clearly show that the fast ion mechanism is responsible for sawtooth control it is desirable to attempt to reduce the effect that fast ions have on the magnetic shear. By doing this it was possible to compare favourably with the fast ion control mechanism outlined in Ref. [11], and to remove the possibility that the sawteeth were controlled by a change in

the magnetic shear (as in the ECCD experiments described in section III and IV). We summarise here dedicated experiments [20] employing minority ^3He , with resonance placed on the high field side close to r_1 . These experiments are also important because minority ^3He is expected to be used routinely in ITER.

The gross fast ion current density $j_h = en_h Z_h v_h$, where v_h is the v_{\parallel} moment of the distribution function. However, the plasma is dragged along with the fast ions, such that the total current is proportional to a drag coefficient j_d , so that $j_{tot} = j_h \times j_d$. The fast ion current is subject to momentum conservation, quasi-neutrality and the balance of collision rates of electrons on all ion species [45], giving

$$j_d = 1 - \left[\frac{Z_h}{Z_{eff}} + \frac{m_h \sum_i Z_i n_i (1 - Z_i/Z_{eff})}{Z_h \sum_i n_i m_i} - G \left(\frac{Z_h}{Z_{eff}} - \frac{m_h \sum_i n_i Z_i^2}{Z_h Z_{eff} \sum_i n_i m_i} \right) \right],$$

where $G = 1.46A(Z_{eff})\epsilon^{1/2}$, A is a weak function of Z_{eff} and i denotes ion species other than hot (h). Due to the minority ion mass number $m_h = 3$ and charge $Z_h = 2$ and moderate $Z_{eff} \approx 1.8$ giving $A \approx 1.4$, the effect of the plasma drag on ^3He minority is to reverse the sign of the net current density inside $q = 1$, and to neutralise the current density and the change in the shear at $q = 1$. Thus, it is seen that the driven current for ^3He minority ICRH is very small, or even in reverse. For this reason, it was suggested by Bhatnagar *et al* [6] that sawtooth control using localised ICRH with minority ^3He would not work. However, as discussed in some detail in Ref. [20], the fast ion mechanism devised in Ref. [11] is independent of the driven current.

A particular configuration was chosen which permitted the ^3He resonance to access a $q=1$ radius which was not compromised in size [20]. The two pulses summarized in Fig. 8, reproduced from [20], had the slowest field and current ramp, and the clearest sawtooth control signatures. The field was varied from 2.9 T to 2.96 T. The pulses were identical, except crucially, 78737 employed 4.5MW of counter-propagating waves (-90°), while 78739 employed 4.5MW of co-propagating waves ($+90^\circ$). Also shown in Fig. 8 is the NBI power, the core central electron temperature, the sawtooth period and the $n = 1$ magnetics amplitude for both pulses. All of these signals show the contrasting effects of the antenna phasing on

the sawteeth (and internal kink instability in the case of the magnetics signal).

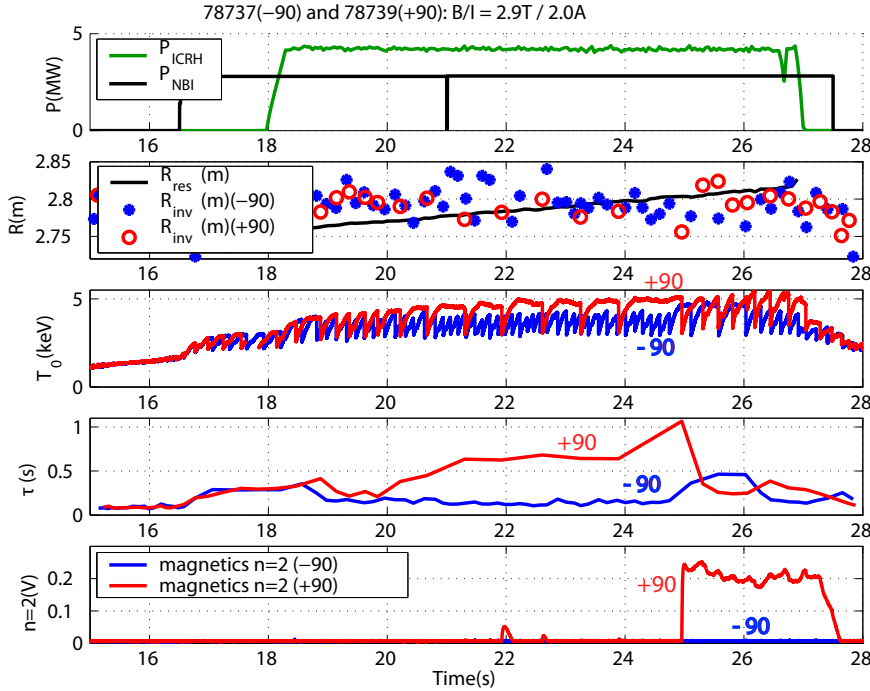


FIG. 8. Time traces of NBI and ICRH power, ^3He resonance position and inversion radius, central electron temperature, sawtooth period and $n = 2$ magnetics amplitude for pulses 78737 (blue, -90° phasing) and 78739 (red, $+90^\circ$ phasing). Figure reproduced from [J. P. Graves, *et al* Nucl. Fusion **50**, 052002 (2010), copyright 2010 Euratom].

The minority ion concentration was less than 1 percent, giving large fast ion tail temperatures. Sawteeth were strongly affected when the resonance was close to the inversion radius (r_{inv}). Discharge 78737 (-90°) demonstrates sawtooth destabilisation (small period) as the resonance position is varied over a width of a few percent of the plasma minor radius. For 78739 ($+90^\circ$), when the resonance position was sufficiently close to the $q = 1$ radius, the sawteeth became so long that a neoclassical tearing mode was triggered. This occurred despite being in L-mode, with normalised beta of around 0.8. The two pulses in Fig. 8 clearly demonstrate the importance and feasibility of sawtooth control. It is pointed out here that it was possible to reproduce the signatures of the sawteeth (with respect to magnetic field variation) on demand. **As discussed in Ref. [20], the sensitive dependence of sawtooth period with respect to resonance position, and the opposing**

dependence for plus and minus 90° phasing, is explained consistently by the fast ion mechanism proposed in Ref. [11]. Moreover, deliberate increase in the ^3He concentration enabled the effect on sawteeth to disappear, which was expected due to the reduced finite orbit width [20]. It was argued in Ref. [20] that these experiments, planned in advance from the predictions of the model, lent strong empirical support for the proposed mechanism, especially as the driven current would not be worsened by the moderate increase in ^3He concentration. While the ^3He pulses have removed the possibility of the influence of driven current, the two antenna configurations yield different fast ion pressure profiles due to the pinch effect described and observed previously in JET [16]. As a result, the kinetic contribution of trapped ions [13] is different for the two cases, and this is indeed accounted for self-consistently in the analysis and simulations of Ref. [20]. Nevertheless, the SELFO [46] calculated inward pressure pinch for the $+90^\circ$ pulse (76190), and outward pinch for the -90° pulse (76189), simply leads to a small radial shift in the collisionless trapped ion response as the resonance position is varied relative to r_1 , and thus cannot explain the narrow peak in $|\delta W|$, and certainly not the sign of δW (peak for $+90^\circ$, trough for -90°). It is clear, however, that at a more fundamental level, the pressure pinch effect [16] and the asymmetry effect on sawteeth [11] are related in the sense that they are a consequence of toroidal wave propagation and finite orbit widths.

VIII. CONCLUSIONS

This paper attempts to bring together some of the primary sawtooth control experiments conducted over recent years. The work presented here is of relevance to experiments in burning plasmas where it is expected that long sawteeth may trigger confinement degrading NTMs, which in some cases may lead to disruption. It has been shown that real-time control of the deposition of the ECH resonance can be exploited in order to achieve real-time control

of the sawtooth in both TCV and TORE-SUPRA. That sawteeth can be controlled in TORE-SUPRA even when there is a substantial fast ion content is particularly encouraging for ITER where it is expected that alpha particles will otherwise lengthen sawteeth. For this reason, the present contribution also attempts to calculate the expected contribution of the ECH launchers to the magnetic shear at $q = 1$. In the ITER simulations, it is shown that the shear can be significantly modified by ECCD. However, it is as yet unclear whether this effect will be sufficient to overcome the alpha particle stabilisation.

A contrasting means of controlling sawteeth is through the direct non-MHD effects brought about by collisionless fast ions, either NBI ions or RF ions. A selection of JET experiments demonstrate that by deliberate manipulation of the fast ion distribution function, it is possible to control sawteeth without the requirement of magnetic shear modification. It is hoped that with these techniques it might be possible to counter the stabilising effect of alpha particles in a more direct way. Before ITER operations commence, it should be possible to conduct more experiments, and perform more analysis and simulations to test whether this is feasible. Indeed, ITER will have real-time capability over both ECH and ICRH actuators. Such studies are ongoing.

Finally, the experimental results presented here are a subset of successful experimental techniques. Sawteeth are generally extremely sensitive to the parameterisation of their actuators. Nevertheless, via improving theoretical understanding, and advanced real-time techniques, it is now becoming possible to routinely control sawteeth. The challenge now is to repeat these techniques with large stabilising trapped ion populations in the core, and in H-mode. Such experiments have been conducted in JET and will be published in due course, but more experiments, theory and simulations are required in order to judge the capability of sawtooth control techniques in future burning tokamaks.

Acknowledgements: The authors of this work are grateful to B. Alper, M. de Baar, K. Crombe, L.-G. Eriksson, R. Felton, D. Howell, V. Kiptily, H. R. Koslowski, M.-L. Mayoral,

I. Monakhov, I. Nunes, S. D. Pinches. This work, supported by the Swiss National Science Foundation, and by the European Communities under contract of Association between EU-RATOM and Confédération Suisse, was carried out within the framework of the European Fusion Development Agreement. The views and opinions expressed herein do not necessarily reflect those of the European Commission.

REFERENCES

- [1] ITER Physics Basis Editors *et al.*, Nucl. Fusion **39**, 2137, (1999).
- [2] D. J. Campbell, D. F. H. Start, J. A. Wesson, D. V. Bartlett *et al*, Phys. Rev. Lett. **60** 2148 (1988).
- [3] O. Sauter, E. Westerhof, M. L. Mayoral, B. Alper *et al*, Phys. Rev. Lett. **88**, 105001 (2002).
- [4] I. T. Chapman, S. Coda, S Gerhardt, J.P. Graves, D. F. Howell, A. Isayama, R. J. La Haye, Y. Liu, P. Maget, M. Maraschek, S. Sabbagh, O. Sauter, submitted to Nucl. Fusion
- [5] F. Romanelli, *Nuc. Fusion* **49**, 104006 (2009)
- [6] V.P. Bhatnagar *et al*, Nucl. Fusion **34**, 1579 (1994).
- [7] L. -G. Eriksson *et al*, Phys. Rev. Lett. **92**, 235004 (2004)
- [8] L.-G. Eriksson *et al*, Nucl. Fusion **45**, S951 (2006).
- [9] M. Mantsinen, *et al*, Plasma Phys. and Control. Fusion **44**, 1521 (2002)
- [10] J. P. Graves, Phys. Rev. Lett. **92**, 185003 (2004)
- [11] J. P. Graves, *et al*, Phys. Rev. Lett. **102**, 065005 (2009)
- [12] C. K. Phillips J. Hosea, E. Marmor, M. W. Phillips *et al*, Phys. Fluids B **4**, 2155 (1992)
- [13] R. B. White, *et al*, Phys. Rev. Lett. **60**, 2038 (1988)
- [14] J. W. Connor and J. G. Cordey, Nucl. Fusion **14**, 185 (1974)
- [15] T. Hellsten *et al*, Phys. Rev. Lett. **74**, 3612 (1995)
- [16] L.-G. Eriksson *et al*, Phys. Rev. Lett. **81**, 1231 (1998)
- [17] I. T. Chapman, *et al*, Plasma Phys. Control. Fusion **50**, 045006 (2008)

- [18] J. I. Paley , *et al*, Plasma Phys. Control. Fusion **51**, 124041 (2009)
- [19] M. Lennholm, *et al* Phys. Rev. Lett. **102**, 115004 (2009)
- [20] J P. Graves, *et al*, Nuclear Fusion **50**, 052002 (2010)
- [21] A. Ekedahl, *et al* Nucl. Fusion **38**, 1397 (1998)
- [22] S. Wukitch, *et al* Phys. Plasmas **12** 056104 (2005)
- [23] I. T. Chapman, *et al* submitted to Plasma Phys. Control. Fusion
- [24] H. Reimerdes *et al.*, Plasma Phys. Control. Fusion **42**, 629 (2000).
- [25] S. Migliuolo, F. Pegoraro and F. Porcelli, Phys. Fluids B **3**, 1338 (1991); L. Zakharov, B. Rogers and S. Migliuolo, Phys. Fluids B **5**, 2498 (1993).
- [26] F. Porcelli, D. Boucher and M. N. Rosenbluth, Plasma Phys. Controlled Fusion **38**, 2163 (1996).
- [27] F. M. Levinton, L. Zakharov, S. H. Batha, J. Manickam and M. C. Zarnstorff, Phys. Rev. Lett. **72**, 2895 (1994).
- [28] O. Sauter *et al*, 1999 Theory of Fusion Plasmas: Proc. Joint Varenna-Lausanne Int. Workshop (Varenna, 1998) ed J.W. Connor et al ISPP-18 (Bologna: Editrice Compositori) p 403
- [29] J. P. Graves, *et al*, Phys. Plasmas **17**, 056118 (2010)
- [30] C. Angioni, *et al*, Nucl. Fusion **43**, 355 (2003)
- [31] M. Lennholm, *et al*, Fusion Sci. and Tech. **55**, 45 (2009)
- [32] M. Lennholm, in preparation for publication
- [33] L-G. Eriksson, *et al*, Phys. Rev. Lett. **92**, 235004 (2004)
- [34] S. Coda, L.-G. Eriksson, M. Lennholm, J. P. Graves, T. Johnson, J. H. Brzozowski, M.

- DeBaar, D. F. Howell, S. Jachmich, V. Kiptily, R. Koslowski, M.-L. Mayoral, A. Mueck, S. Pinches, G. Saibene, M. I. K. Santala, M. F. Stamo, M. Valisa and JET-EFDA contributors, Proceedings of Contributed Papers, 34th European Physical Society Plasma Physics Conference, Warsaw, 2007, edited by Pawel Gasior and Jerzy Wolowski, International Conference on Plasma Physics, Omsk, 1986, edited by I. I. Ivanovich, Vol. 31F, P5.130.
- [35] M. Henderson et al., in Proc. of the 21st IAEA Fusion Energy Conference, Chengdu, China (IAEA, Vienna, 2006), Vol. IT/P2-15.
- [36] Zucca C 2009 PhD Thesis EPFL, no 4360 <http://library.epfl.ch/en/theses/?nr=4360>
- [37] I. T. Chapman *et al*, Nucl. Fusion **50**, 035006 (2009).
- [38] M. F. F. Nave, Phys Plasmas **13**, 014503 (2006)
- [39] J. P. Graves, *et al*, Plasma Phys. Control. Fusion **47**, B121 (2005)
- [40] I. T. Chapman, T. C. Hender, S. Saarelma, S. E. Sharapov, R. J. Akers and N. J. Conway, Nucl. Fusion **46** 1009 (2006)
- [41] I. T. Chapman, S. D. Pinches, H. R. Koslowski, Y. Liang, A. Kramer-Flecken and M. de Bock, Nucl. Fusion **48** 035004 (2008).
- [42] J. P. Graves, R. J. Hastie and K. I. Hopcraft, Plasma Phys. Control. Fusion **42**, 1049 (2000).
- [43] J. P. Graves *et al*, Phys. Plasmas **12**, 090908 (2005).
- [44] I. T. Chapman *et al*, Phys. Plasmas, **14**, 070703 (2007)
- [45] N. J. Fisch *et al*, Rev. Mod. Phys. **59**, 175 (1987).
- [46] J. Hedin, *et al*, Nucl. Fusion **42**, 527 (2002).